

operant conditioning to train them on a memory task, giving a juice reward during training sessions. The monkeys sat in a primate chair 30 cm from a computer colour monitor equipped with a touch screen (31.5 cm × 26.5 cm). Trial events, stimulus presentation and data recording were computer controlled.

Behavioural shaping

The monkeys learned to press a lever following onset of a fixation spot and not to release it during presentation of three sample stimuli. At first, the stimuli in each sample presentation were chosen randomly (without repetitions) from the whole image set of 30 images. During the test phase of the trial, the same three stimuli were displayed on the screen simultaneously. This served as a 'go' signal for the monkeys to release the lever and touch the images on the screen. A touch of each image made in any order was rewarded, but repeated touches of the same image were considered as errors. During a brief final period of the shaping (monkey J: 100 trials; S: 400 trials; R: 700 trials) a fourth distractor image was added to the test stimulus, with the monkeys still rewarded irrespective of the order of touches, as long as they avoided repeated touches or touching the distractor.

In the tested behavioural task (described below), sample stimuli were shown as fixed ordered triplets and the image touches were rewarded only if they were made in the order of sample image presentation.

Stimuli

Thirty fractal images were presented repeatedly in a fixed temporal order, divided into ten constant non-overlapping triplets (A1, A2, A3; B1, B2, B3; ...; J1, J2, J3; A1, A2, A3; ...). Each trial consisted of a triplet of three sample stimuli, with each stimulus having a fixed ordinal position in its triplet (first, second or third). During each trial, a single triplet was displayed twice: first, sequentially, during the sample sequence and then, simultaneously, during the test presentation. A distractor stimulus, randomly chosen from the remaining 27 images, was added to the test presentation of the triplet (Fig. 1a, b).

Behavioural task

Monkeys were trained on a novel delayed sequence recall (DSR) task. The basic DSR task is shown schematically in Fig. 1b. Following presentation of a fixation spot on the screen, the monkey pressed a lever. This initiated presentation of a series of three sample stimuli (a triplet) in a fixed temporal order. Each sample image was presented at the centre of the screen for 500 ms with a 1 s inter-stimulus interval. Finally, the three sample images were presented together with a fourth, distractor stimulus at random positions on the screen. This test display served as a 'go' signal for the monkey to release the lever and touch the three sample images on the screen in the order of their previous presentation, without touching the distractor. Touching a wrong image ended the trial, whereas each correct touch was rewarded with juice. The third correct touch completing the trial was rewarded with a larger portion of juice. The number of trials per session varied considerably from session to session (between 17 and 269 trials). The monkeys were allowed to perform as many trials as they wished in a given session.

Task variations

After a period of prolonged training on the basic task, the monkeys were tested on additional task paradigms to study the role of different memory strategies on task performance:

(1) Trials with no samples (task NS): In this task variant, we tested touch-order behaviour without presentation of the initial sample stimuli. During each of the 'sample' viewing times, the monkeys were presented with a grey rectangle, to maintain the temporal structure of the task.

(2) Trials with stimuli shuffled between triplets but within categories (SH): In this variant the stimuli within each category were shuffled to form new triplets on each trial. Thus the shuffling maintained the ordinal category of each stimulus, but destroyed the original fixed order of the whole set. The same shuffled stimuli were presented in the test phase.

(3) Trials with no samples and shuffled stimuli (NS+SH). We combined the two previous manipulations, shuffled the stimuli and displayed them only once, during the 'test' presentation. Reward was contingent only on touching the correct category.

Received 29 September 1999; accepted 4 January 2000.

1. Terrace, H. The phylogeny and ontogeny of serial memory: List learning by pigeons and monkeys. *Psychol. Sci.* **4**, 162–169 (1993).
2. Ebbinghaus, H. *Memory: A Contribution to Experimental Psychology* (Dover, New York, 1964 (1885)).
3. Young, R. K. The stimulus in serial verbal learning. *Am. J. Psychol.* **74**, 517–528 (1961).
4. Ebenholtz, S. in *The Psychology of Learning and Motivation* (ed. Bower, G.) 267–314 (Academic, New York, 1972).
5. D'Amato, M. & Colombo, M. Representation of serial order in monkeys (*Cebula apella*). *J. Exp. Psychol. Anim. Behav. Proc.* **14**, 131–139 (1988).
6. Terrace, H. Chunking by a pigeon in a serial learning task. *Nature* **325**, 149–151 (1987).
7. Swartz, K., Chen, S. & Terrace, H. Serial learning by rhesus monkeys: I. Acquisition and retention of multiple four-item lists. *J. Exp. Psychol. Anim. Behav. Proc.* **17**, 396–410 (1991).
8. McGonigle, B. & Chalmers, M. Monkeys are rational! *Q. J. Exp. Psychol.* **45**, 189–228 (1992).
9. Treichler, F. & van Tilburg, D. Concurrent conditional discrimination tests of transitive inference by macaque monkeys: List linking. *J. Exp. Psychol. Anim. Behav. Proc.* **22**, 105–117 (1996).
10. Straub, R. O. & Terrace, H. S. Generalization of serial learning in the pigeon. *Anim. Learn. Behav.* **9**, 454–468 (1981).
11. Terrace, H. S. A non-verbal organism's knowledge of ordinal position in a serial learning task. *J. Exp. Psychol. Anim. Behav. Proc.* **41**, 203–214 (1986).
12. Terrace, H., Chen, S. & Newman, A. Serial learning with a wild card by pigeons: Effect of list length.

J. Comp. Psychol. **109**, 162–172 (1995).

13. D'Amato, M. & Colombo, M. Serial learning with wild card items by monkeys (*Cebus apella*): implications for knowledge of ordinal position. *J. Comp. Psychol.* **103**, 252–263 (1989).
14. D'Amato, M. & Colombo, M. The symbolic distance effect in monkeys (*Cebula apella*). *Anim. Learn. Behav.* **18**, 133–140 (1990).
15. Chen, S., Swartz, K. B. & Terrace, H. S. Knowledge of the ordinal position of list items in rhesus monkeys. *Psychol. Sci.* **8**, 80–86 (1997).
16. Sands, S. F. & Wright, A. A. Serial probe recognition performance by a rhesus monkey and a human with 10- and 20-item lists. *J. Exp. Psychol. Anim. Behav. Proc.* **6**, 386–396 (1980).
17. Gower, E. Short-term memory for the temporal order of events in monkeys. *Behav. Brain Res.* **52**, 99–103 (1992).
18. Murray, E. I., Gaffan, D. & Mishkin, M. Neural substrates of visual stimulus-stimulus association in rhesus monkeys. *J. Neurosci.* **13**, 4549–4561 (1993).
19. Sakai, K. & Miyashita, Y. Neural organization for the long-term memory of paired associates. *Nature* **354**, 152–155 (1991).
20. Naya, Y., Sakai, K. & Miyashita, Y. Activity of primate infero-temporal neurons related to a sought target in pair-association task. *Proc. Natl Acad. Sci. USA* **93**, 2664–2669 (1996).
21. Buffalo, B. & Gaffan, D. A primacy effect in monkeys when list position is relevant. *Q. J. Exp. Psychol.* **47B**, 353–369 (1994).
22. Farrar, D. N. Picture memory in the chimpanzee. *Percept. Motor Skills* **25**, 305–315 (1967).
23. Mishkin, M. A memory system in the monkey. *Phil. Trans. R. Soc. Lond.* **298**, 83–95 (1982).
24. Fuster, J. *The Prefrontal Cortex: Anatomy, Physiology and Neurophysiology of the Frontal Lobe* (Raven, New York, 1989).
25. Colombo, M., Eickhoff, A. E. & Gross, C. G. The effects of inferior temporal and dorsolateral frontal lesions on serial-order behavior and visual imagery in monkeys. *Cogn. Brain Res.* **1**, 211–217 (1993).
26. Petrides, M. Impairments on nonspatial self-ordered and externally ordered working memory tasks after lesions of the mid-dorsal part of the lateral frontal cortex in the monkey. *J. Neurosci.* **15**, 359–375 (1995).
27. Parker, A. & Gaffan, D. Memory after frontal/temporal disconnection in monkeys: conditional and non-conditional tasks, unilateral and bilateral frontal lesions. *Neuropsychologia* **36**, 259–271 (1998).

Acknowledgements

We thank D. Amit for insightful theoretical discussions and many practical suggestions during the course of these experiments, and S. Fusi, M. Dvorkin and O. Algaoy for computer assistance. This study was supported by grants from the Israel Science Foundation of the Academy of Arts and Sciences, the McDonnell-Pew Science Foundation and the US–Israel Binational Science Foundation (BSF). T.O. and V.Y. were supported in part by the Israel Ministry of Absorption.

Correspondence and requests for materials should be addressed to T.O. (e-mail: tanyao@apollo.is.huji.ac.il).

Temporal patterns of human cortical activity reflect tone sequence structure

Aniruddh D. Patel* & Evan Balaban*

The Neurosciences Institute, 10,640 John Jay Hopkins Drive, San Diego, California 92121, USA

* These authors contributed equally to this work

Despite growing interest in temporal aspects of auditory neural processing^{1,2}, little is known about large-scale timing patterns of brain activity during the perception of auditory sequences³. This is partly because it has not been possible to distinguish stimulus-related activity from other, endogenous brain signals recorded by electrical or magnetic sensors. Here we use amplitude modulation of unfamiliar, ~1-minute-long tone sequences to label stimulus-related magnetoencephalographic neural activity in human subjects^{4–9}. We show that temporal patterns of activity recorded over particular brain regions track the pitch contour of tone sequences, with the accuracy of tracking increasing as tone sequences become more predictable in structure. In contrast, temporal synchronization between recording locations, particularly between sites over the left posterior hemisphere and the rest of the brain, is greatest when sequences have melody-like statistical properties^{10,11}, which may reflect the perceptual integration of local and global pitch patterns in melody-like

sequences¹². This method is particularly well suited to studying temporal neural correlates of complex auditory sequences (such as speech or music) which engage multiple brain areas as perception unfolds in time.

Five male human subjects heard sequences of pure tones while neuromagnetic signals were recorded using a 148-channel whole-head biomagnetometer (Biomagnetic Technologies). We took advantage of the fact that continuous amplitude modulation of tones results in detectable cortical activity at the modulation frequency, termed the 'steady-state response' (SSR)^{4–6}. The SSR is strongest when amplitude modulation is in the 40-Hz region⁷, and it may originate from two or more sources in each primary auditory cortex (Heschl's gyrus)^{8,9}. We applied a constant 41.5-Hz amplitude modulation (constant 'modulating frequency') to tone sequences (with varying 'carrier frequency') to identify cortical activity that was directly related to the stimulus. Listeners heard these stimuli as sequences of carrier-frequency pitches, and generated a robust SSR at 41.5 Hz whose timing (phase) varied as a function of the carrier frequency of the underlying tones (Fig. 1a–e).

Each subject heard 28 1-min tone sequences drawn from four structural categories. All categories used 415-ms-long pitches from

25 frequencies that were logarithmically equally spaced between 220 and 880 Hz (between musical A3 and A5 in semitone steps). We used a method of generating novel, unfamiliar stimuli in which different members of the same stimulus category were structurally unique, but shared common statistical properties¹³. The four structural categories differed in the relative balance of long-term pitch trends versus rapid point-to-point fluctuations (Fig. 1f–i, dashed black lines), which was controlled by specifying the slope of the pitch–time series power spectrum. In the first category, pitch–time patterns had a flat power spectrum corresponding to random variation from one pitch to the next. In the next two categories, pitch–time patterns had spectra with slopes of around $1/f$ and $1/f^2$, respectively, leading to two different 'fractal' patterns of constrained variation that more closely resembled musical melodies^{10,11,14,15}. The final category had deterministic pitch–time patterns consisting of linear step-wise motion up and down musical scales. Subjects were exposed to exemplars of the pitch patterns in a brief training session. Even though no information was given apart from examples and their category numbers (1 to 4), subjects had little difficulty forming perceptual categories and discriminating between the stimuli, as shown previously¹³. During the experiment, subjects identified the category number of each sequence after its presentation with few errors. With the exception of the scale pattern, every stimulus in the training session and experiment was unique, meaning that subjects discriminated the stimuli on the basis of statistical properties rather than by memorizing particular features.

For each trial in a given subject, data from each sensor were segmented into 2-s epochs and fast Fourier transformed to examine the magnitude and phase of the neuromagnetic signals in a 0.5-Hz band centred at 41.5 Hz. This gave energy (magnitude²)–time and phase–time series for each sensor. When the phase–time series were unwrapped and detrended (see Methods), recordings from particular sensor positions showed a marked resemblance to the contour of the pitch–time series heard by the subject (Fig. 1f–i, solid red lines). Energy–time series (the amplitude of the SSR response over time) never showed this pattern. For a given subject, sensor locations whose phase–time series showed a nominally significant positive correlation with the pitch–time series at the $P \leq 0.05$ level (one-tailed test) on >25% of all trials were designated 'tracking locations'. These locations had a consistent bilateral spatial distribution in all subjects, with a statistical tendency for their density to be greater on the right side across all subjects (Fig. 2a, 42 left compared with 83 right, χ^2 value relative to a symmetric distribution = 6.884, $P = 0.0102$, Fisher exact test¹⁶). When tracking performance was compared across the four stimulus categories at these locations, each subject showed highly significant differences in tracking between the categories (all $P < 0.0001$, Kruskal–Wallis analysis of variance (ANOVA)¹⁶). The correlation between neuromagnetic phase–time and stimulus pitch–time contours increased in the order random < $1/f < 1/f^2 < scales$ in all subjects (Fig. 2c). Across subjects, this pattern of increasing correlation with increasing stimulus structure was highly significant (Friedman two-way ANOVA¹⁶, $\chi^2 = 15.00$, d.f. = 3, $P = 0.0018$).

Energy changes in the neuromagnetic signal did not track stimulus structure. For each subject, baseline energy was computed in a 0.5-Hz band centred at 41.5 Hz for each channel over at least 50 2-s silent epochs recorded before the onset of stimulus presentations. Sensor locations where mean energy exceeded baseline by more than 1.96 s.d. on >25% of all trials were designated 'energy locations'. Energy and tracking locations overlapped in each subject, though one did not completely predict the other (Fig. 2b). No subject showed significant differences in energy between conditions at their energy locations (Kruskal–Wallis ANOVA, all $P > 0.25$, Fig. 2d). This suggests an aspect of the neural response that is actively related to the presence of an auditory stimulus but which does not vary with the structure of pitch–time sequences.

Our observations of cortical phase tracking of pitch sequences,

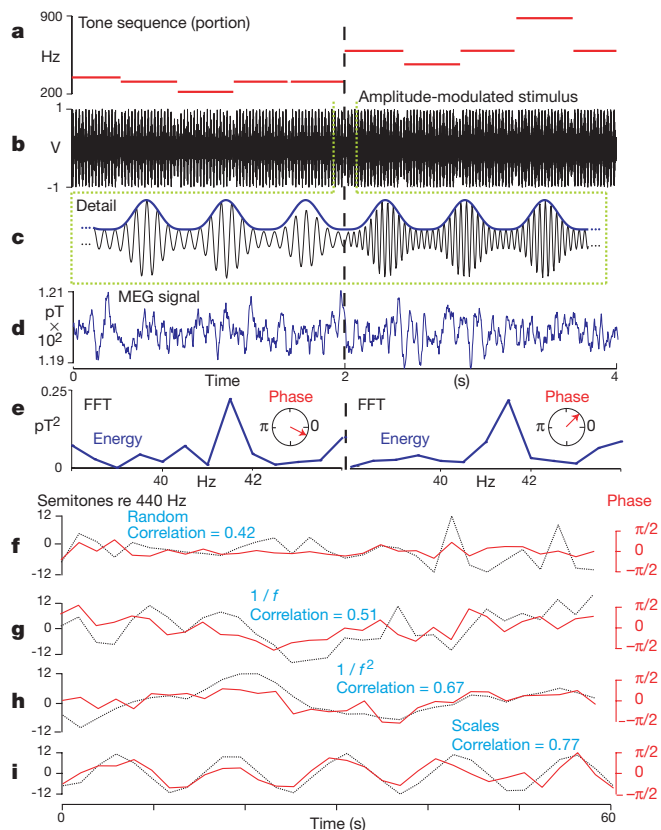


Figure 1 Phase tracking of tone sequences by the human brain. **a–d**, Stimulus and brain response over 4 s. **a**, Tone frequencies; **b**, stimulus waveform; **c**, waveform detail (150 ms), showing constant modulating frequency (purple) overlaid on changing carrier frequency (black); **d**, neural signal from one sensor (MEG, magnetoencephalography). **e**, Successive 2-s spectra of neural signal. The SSR has an energy peak at 41.5 Hz (purple), whose phase (red arrow) varies with carrier frequency. FFT, fast Fourier transform. **f–i**, Phase-tracking of individual tone sequences. Pitch–time contours (dotted black lines) illustrate the four different stimulus categories. Associated neuromagnetic phase–time series (solid red lines) from a single sensor during one trial in one subject were randomly drawn from the top 10% of sensor correlation values for each stimulus category. The correlation between the resampled pitch–time series and the neuromagnetic phase–time series is given in the inset to each graph. Tone sequences can be heard in the Supplementary information at <http://www.nature.com>.

consistent with earlier suggestions of a dependency between stimulus frequency and SSR phase⁴, have uncovered unexpectedly strong phase tracking over extended times, and a relationship between the quality of tracking and the statistical structure of pitch sequences. Although such tracking may depend upon frequency-dependent delays introduced in the cochlea⁴ and expanded on the way to the cortex¹⁷ these are unlikely to account for the modulation of tracking by pitch-sequence structure. This phenomenon may be due to a modulation of the number, phase synchrony or mean activity level of cells in the phase-tracking populations and/or a modulation of phase-noise in the 41.5-Hz frequency region by differential activity of cells which respond to the stimulus but are not involved in phase tracking. Modulation of these populations may originate from cortical and/or subcortical sites. Additional work is required to distinguish between these possibilities.

We also investigated the relationship between the statistical structure of pitch sequences and large-scale patterns of interaction among brain regions in the 41.5-Hz frequency band containing stimulus-related activity. Interactions were quantified in terms of phase coherence, a measure of temporal synchronization between pairs of sensors during a particular condition. To minimize the role of common neural sources, we included only sensor pairs >12 cm apart, as determined by regression analysis of coherence on inter-sensor distance for each subject¹⁸ (see Supplementary information). Phase coherences were computed for all such sensor pairs within each subject and condition after concatenating data for all seven trials. To remove the effects of absolute differences in sensor phase coherence and focus on changes between conditions, sensor interactions were classified by recording region (anterior left, anterior right, posterior left, posterior right) and type (tracking locations, non-tracking locations) and normalized within each subject (see Methods). The patterns of normalized phase coherence variation

among the four conditions were then combined across all subjects to investigate the significance of general and regional trends.

Across all subjects and brain areas a general trend emerged (Fig. 3a, Kruskal–Wallis ANOVA, d.f. = 3, $H = 499.6$, $P < 0.0001$, all post-hoc multiple comparisons significantly different at the 0.05 level). Random pitch sequences generated less coherence than the other, more patterned sequences, and $1/f^2$ sequences generated more coherence than deterministic scale patterns or $1/f$ sequences. Statistical research on Western musical pieces suggests that their pitch–time sequences have power spectra which are about $1/f^2$ (refs 10, 11), suggesting that music-like sequences generated the greatest synchronization between recording locations.

To investigate large-scale regional spatial patterns in coherence data, we segregated phase coherences according to the scheme shown in Fig. 3b. The general pattern in Fig. 3a reappears in the interactions between sensors above the posterior left brain hemisphere and those over the rest of the brain, which accounted for 45.6% of all sensor comparisons (Fig. 3c, Kruskal–Wallis ANOVA, $H = 173.4$, 33.7, 91.2, all $P < 0.0001$ for interactions vii, viii and ix, respectively; $1/f^2$ sequences show significantly greater coherence than the other conditions in post-hoc multiple comparisons at the 0.05 level). In contrast, in the remaining inter-regional comparisons (43.4% of comparisons) $1/f$ and $1/f^2$ sequences showed equivalent phase coherence (Fig. 3d, Kruskal–Wallis ANOVA, $H = 124.1$, 147.752, 157.5, all $P < 0.0001$ for interactions v, vi and x, respectively). Comparisons within the four regions (11% of all sensor comparisons) showed no consistent trends in their pattern of variation (Fig. 3e).

Imaging studies of music based on metabolic measures¹⁹ have largely implicated right fronto-temporal circuits in melodic processing. Studies of brain-damaged patients indicate that left superior temporal areas may be involved in the processing of local

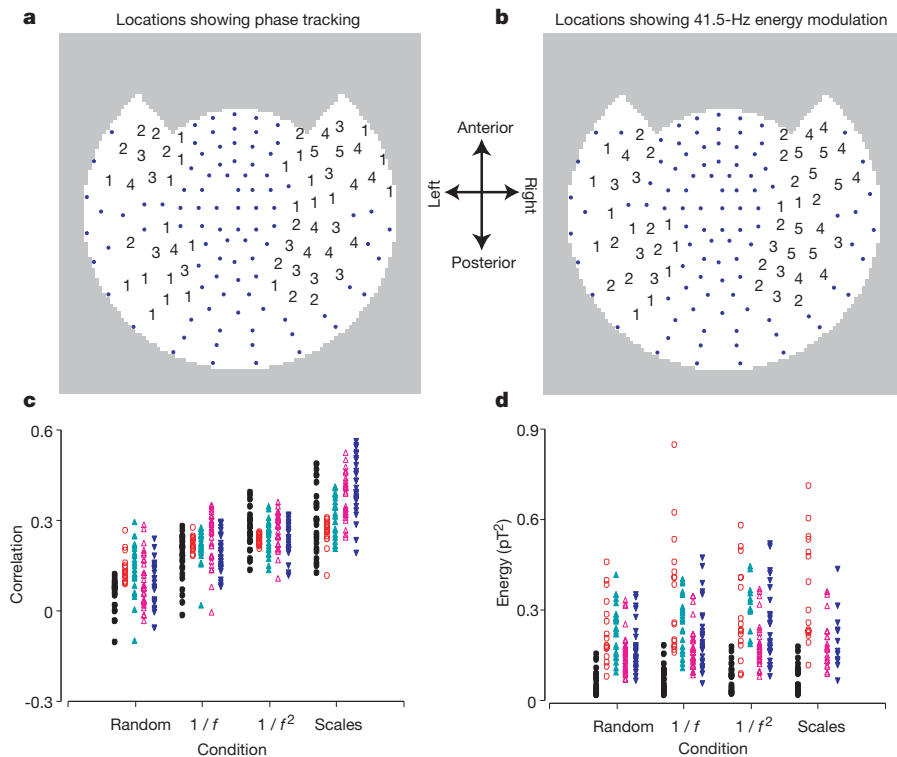


Figure 2 Topographic distribution of sensor locations. **a**, Locations where phase covaried with tone frequency; **b**, locations where responses showed energy modulation at 41.5 Hz. Numbers indicate how many subjects (out of five) at each sensor location exceeded phase-tracking criteria (**a**) and energy-threshold criteria (**b**). Dots indicate locations that did not meet these criteria. **c**, Correlations between tone frequency and

response phase for the four types of sequence. Each data point represents the mean correlation over seven trials for one type of tone sequence for one subject at one phase-tracking sensor location. Each subject is shown with a single colour/shape combination. **d**, Mean 41.5-Hz energy at energy locations as a function of stimulus condition; symbols as in **c**.

melodic intervals in musical sequences, whereas right fronto-temporal circuits are involved in the perception of global pitch contour^{12,20}. Our data point to a potential neural correlate of the perceptual integration of local and global pitch information, and suggest that this integration is maximal for melody-like sequences. Dynamic imaging techniques can thus provide an important complement to metabolic imaging (such as functional magnetic resonance imaging or positron emission tomography) in the mapping of brain activity associated with music perception.

Auditory steady-state responses to amplitude-modulated sounds have been studied by a number of researchers interested in both the tonotopic organization of human auditory cortex^{5,21} and mechanisms of cortical signal generation^{6–8,22}. Such studies have typically used repetitive stimuli and extensive time-domain averaging to detect brain responses or to localize their sources. Our approach provides complementary information by elucidating dynamic temporal aspects of neural responses. This technique is especially suitable for the continuously changing sequences that are ubiquitous in speech and music, as well as for studying dynamic interactions between hearing and other sensory modalities such as vision. □

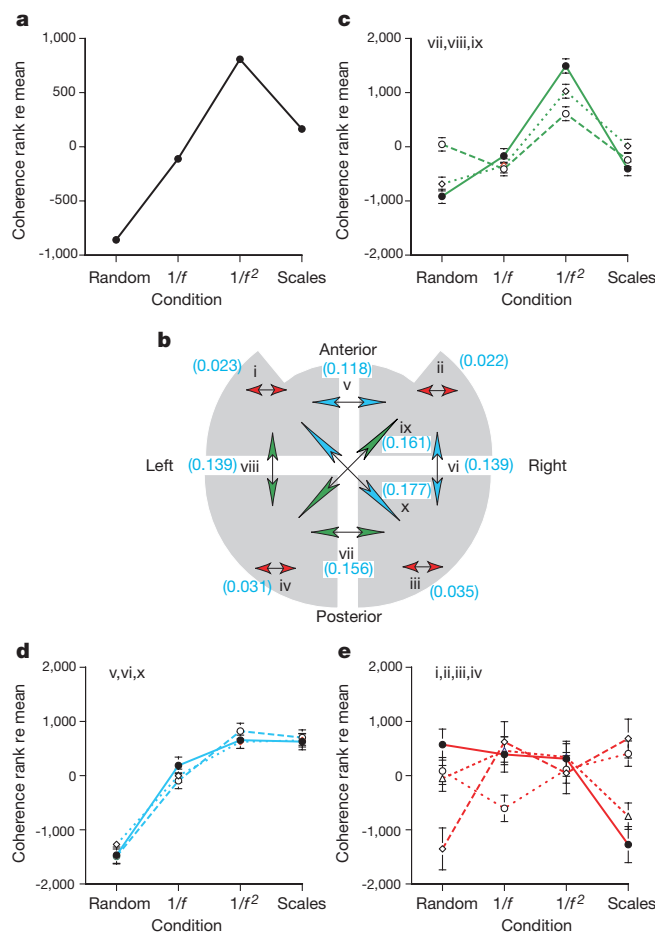


Figure 3 Changes in brain interactions among the four stimulus conditions. Graphs illustrate differences in mean ranks across conditions (error bars ± 1 s.e.m.; no bars, s.e.m. smaller than data point symbol). **a**, General pattern of coherence rank changes across all regions and subjects. **b**, Subdivision of brain regions into four quadrants (i, ii, iii, iv: sensor pairings within each quadrant; v–x: interregional interactions indicated by the neighbouring arrows). Numbers in parentheses: proportion of total sensor-pair interactions represented by each grouping. **c**, Inter-regional interactions involving sensors over the posterior left region: filled circle, vii; open circle, viii; open diamond, ix. **d**, Remaining inter-regional interactions: filled circle, v; open circle, vi; open diamond, x. **e**, Intra-regional interactions: filled circle, i; open diamond, ii; open triangle, iii; open circle, iv.

Methods

Stimulus preparation and presentation

Each tone sequence was created using SIGNAL (Engineering Design), by inverse-Fourier transforming complex spectra whose squared magnitudes declined with frequency at a rate of $1/f^b$, ($b = 0, 1.3$ and 2.1 for random, $1/f$ and $1/f^2$, respectively), and whose phases were random. For each sequence, 145 consecutive values were scaled and rounded to between ± 7 , corresponding to steps along Western musical scales (condition 4 consisted of linear ramps between ± 7 , with 150 total elements). Scale steps were converted to semitone steps (± 12 steps from 440 Hz) according to one of seven Western diatonic musical modes (ionian ('major scale'), dorian, phrygian, lydian, mixolydian, aeolian ('minor scale') and locrian; each mode appeared once in each condition). Semitone values were used to synthesize a tone sequence, with one 415-ms pure tone per frequency and no silences between tones (amplitude ± 1 V, last 20 ms of each tone 0.75 V). The entire tone sequence was amplitude-modulated at a rate of 41.5 Hz to a depth of 0.25 of its maximum amplitude using a \cos^2 envelope. Subjects were five right-handed males aged 30–36 who passed an audiometric test (GSI-65 Audiometer, Grayson-Stadler). Two of the subjects had studied music and the others had no special musical training.

Magnetoencephalographic recordings

Whole-head neuromagnetic signals were collected using a Magnes 2500WH MEG system (Biomagnetic Technologies) in a magnetically shielded room. This system provides 148 magnetometer coils (1 cm in diameter) spaced 3 cm apart on an approximately ellipsoidal surface located ~ 3 cm from the scalp surface. Stimuli were delivered over non-magnetic ER30 tubephones (Etymotic Research) at a comfortable level. The sampling rate for data acquisition was 508.63 Hz for one subject and 678.17 Hz for the others. Data were bandpass filtered from 1–100 Hz online during data acquisition.

Data preparation and analysis

Data preparation and analysis were carried out using MATLAB (MathWorks), SYSTAT (SPSS) and STATVIEW (SAS). Magnetoencephalographic data were fast-Fourier transformed in successive 2-s epochs (1,017-point transform for one subject and 1,356-point transform for the other four) and the magnitude and phase component of each Fourier coefficient were extracted at 41.5 Hz. Energy was estimated as the magnitude² in each epoch.

Phase–time series were unwrapped to correct for large jumps in radian phase and detrended (see Supplementary Information). To compare pitch–time and phase–time series, pitch–time series were down-sampled to match the Fourier transform rate of 1 value per 2 s. Correlations between down-sampled pitch–time series and phase–time series for each subject, trial and sensor were carried out after zero-meaning and root-mean-square amplitude normalization of both waveforms.

To analyse brain interactions in each subject, neuromagnetic data from the seven runs of each condition were concatenated end-to-end and Fourier transformed in 2-s epochs (giving ~ 217 epochs per sensor). Phase coherences were calculated as:

$$\gamma_{xy}^2 = \frac{|F_x/M_x * cc(F_y/M_y)|^2}{|F_x/M_x * cc(F_x/M_x)| |F_y/M_y * cc(F_y/M_y)|}$$

where γ_{xy}^2 is the phase coherence between sensors x and y ; F_x and F_y are the complex Fourier-coefficient time series of sensors x and y at 41.5 Hz; M_x and M_y are the real-valued Fourier magnitude time series of sensors x and y ; $*$ is the dot product operator; and cc is the complex conjugation operator²³. Dividing each Fourier coefficient by its magnitude ensures that the resulting measure is only sensitive to phase. A γ_{xy}^2 value of 1 indicates a constant phase difference between sensors x and y throughout a condition, whereas a γ_{xy}^2 value of 0 means a random phase relationship. The phase coherences of all sensors > 12 cm apart (see Supplementary information) in all four stimulus conditions were ranked from smallest to largest. Sensor locations were classed into four quadrants (anterior left, anterior right, posterior left and posterior right), giving 10 spatial comparison categories (four intra-regional comparisons and six inter-regional comparisons). Sensor comparisons were further subdivided into three types: tracking location channels compared with each other, tracking location channels compared with non-tracking location channels, and non-tracking location channels compared with each other, giving 30 categories of phase coherence comparison in the data set for each subject. As we were interested in exploring differences among the four conditions rather than absolute differences among the sensor categories, the coherence rankings within each category were corrected for level differences due to region and type by subtracting the mean value of the category within each subject. Trends were examined by combining these data across all subjects and examining the variation of the corrected coherence ranks with stimulus condition.

Non-parametric statistics were used in all analyses because of the highly non-normal distributions of correlations, coherences and energy values.

Received 22 September; accepted 6 December 1999.

- Cariani, P. A. & Delgutte, B. Neural correlates of the pitch of complex tones. I. Pitch and pitch salience. *J. Neurophysiol.* **76**, 1698–1716 (1996).
- deCharms, R. C. & Merzenich, M. Primary cortical representation of sounds by the coordination of action potential timing. *Nature* **381**, 610–613 (1996).
- Petsche, H., Richter, P., von Stein, A., Etlinger, S. & Filz, O. EEG coherence and musical thinking. *Music Percept.* **11**, 117–152 (1993).
- Galambos, R., Makeig, S. & Talmachoff, P. J. A 40-Hz auditory potential recorded from the human scalp. *Proc. Natl Acad. Sci. USA* **78**, 2463–2647 (1981).
- Romani, G. L., Williamson, S. J. & Kaufman, L. Tonotopic organization of the human auditory cortex. *Science* **216**, 1339–1340 (1982).

6. Pantev, C. *et al.* Relationship of transient and steady-state auditory evoked fields. *Electroenceph. Clin. Neurophysiol.* **88**, 389–396 (1993).

7. Hari, R., Hämäläinen, M. & Joutsiniemi, S. -L. Neuromagnetic steady-state responses to auditory stimuli. *J. Acoust. Soc. Am.* **86**, 1033–1039 (1989).

8. Gutschalk, A. *et al.* Deconvolution of 40 Hz steady-state fields reveals two overlapping source activities of the human auditory cortex. *Clin. Neurophysiol.* **110**, 856–868 (1999).

9. Makeig, S., Jung, T.-P., Bell, A. J., Ghahremani, D. & Sejnowski, T. J. Blind separation of auditory event-related brain responses into independent components. *Proc. Natl Acad. Sci. USA* **94**, 10979–10984 (1997).

10. Nettheim, N. On the spectral analysis of melody. *Interface* **21**, 135–148 (1992).

11. Boon, J. P. & Decroly, O. Dynamical systems theory for music dynamics. *Chaos* **5**, 501–508 (1995).

12. Liégeois-Chauvel, C., Peretz, I., Babai, M., Laguitton, V. & Chauvel, P. Contribution of different cortical areas in the temporal lobes to music processing. *Brain* **121**, 1853–1867 (1998).

13. Schmuckler, M. A. & Gilden, D. L. Auditory perception of fractal contours. *J. Exp. Psychol.: Hum. Percept. Perform.* **19**, 641–660 (1993).

14. Voss, R. F. & Clarke, J. '1/f noise' in music and speech. *Nature* **258**, 317–318 (1975).

15. Voss, R. F. & Clarke, J. '1/f noise' in music: music from 1/f noise. *J. Acoust. Soc. Am.* **63**, 258–263 (1978).

16. Siegel, S. & Castellan, N. J. Jr *Nonparametric Statistics for the Behavioral Sciences* (McGraw Hill, New York, 1988).

17. Greenberg, S., Poeppel, D. & Roberts, T. in *Psychophysical and Physiological Advances in Hearing* (eds Palmer, A., Summerfield, Q., Rees, A. & Meddis, R.) 293–300 (Whurr, London, 1998).

18. Srinivasan, R., Russell, P., Edelman, G. & Tononi, G. Increased synchronization of neuromagnetic responses during conscious perception. *J. Neurosci.* **19**, 5435–5448 (1999).

19. Zatorre, R. J., Evans, A. C. & Meyer, E. Neural mechanisms underlying melodic perception and memory for pitch. *J. Neurosci.* **14**, 1908–1919 (1994).

20. Patel, A. D., Peretz, I., Tramo, M. & Labrecque, R. Processing prosodic and musical patterns: a neuropsychological investigation. *Brain Lang.* **61**, 123–144 (1998).

21. Pantev, C., Roberts, L. E., Elbert, T., Roß, B. & Wienbruch, C. Tonotopic organization of the sources of human auditory steady-state responses. *Hearing Res.* **101**, 62–74 (1996).

22. Ribary, U. *et al.* Magnetic field tomography of coherent thalamocortical 40-Hz oscillations in humans. *Proc. Natl Acad. Sci. USA* **88**, 11037–11041 (1991).

23. Bendat, J. S. & Piersol, A. G. *Engineering Applications of Correlation and Spectral Analysis* (Wiley, New York, 1993).

Supplementary information is available on Nature's World-Wide Web site (<http://www.nature.com>) or as paper copy from the London editorial office of Nature. For additional sound examples, see http://www.nsi.edu/users/patel/tone_sequences.

Acknowledgements

We thank L. Kurelowech for technical assistance, R. Srinivasan for advice and discussions, and S. Makeig, M. Kutas, T. Urbach and S. Hillyard for suggestions. This research was supported by the Neurosciences Research Foundation as part of its research program on Music and the Brain at The Neurosciences Institute.

Correspondence and requests for materials should be addressed to A.D.P. (e-mail: apatel@nsi.edu) or E.B. (e-mail: evan@nsi.edu).

Cannabinoids control spasticity and tremor in a multiple sclerosis model

David Baker*, Gareth Pryce*, J. Ludovic Croxford*, Peter Brown†, Roger G. Pertwee‡, John W. Huffman§ & Lorna Layward||

* Neuroinflammation Group, Department of Neurochemistry, Institute of Neurology, University College London, 1 Wakefield Street, London WC1N 1PJ and the Institute of Ophthalmology, UCL, London EC1V 9EL, UK

† The Medical Research Council Human Movement and Balance Unit, National Hospital for Neurology and Neurosurgery, Queen Square, London, WC1N 3BG, UK

‡ Department of Biomedical Sciences, Institute of Medical Sciences, University of Aberdeen, Foresterhill, Aberdeen AB25 2ZD, UK

§ Department of Chemistry, Clemson University, Clemson, South Carolina 29634-1905, USA

|| Multiple Sclerosis Society of Great Britain and Northern Ireland, 25 Effie Road, London SW6 1EE, UK

Chronic relapsing experimental allergic encephalomyelitis (CREAE) is an autoimmune model of multiple sclerosis¹. Although both these diseases are typified by relapsing-remitting paralytic episodes, after CREAE induction by sensitization to myelin antigens¹ Biozzi ABH mice also develop spasticity and tremor. These symptoms also occur during multiple sclerosis and are difficult to control. This has prompted some patients to find

alternative medicines, and to perceive benefit from cannabis use². Although this benefit has been backed up by small clinical studies, mainly with non-quantifiable outcomes^{3–7}, the value of cannabis use in multiple sclerosis remains anecdotal. Here we show that cannabinoid (CB) receptor agonism using R(+)-WIN 55,212, Δ⁹-tetrahydrocannabinol, methanandamide and JWH-133 (ref. 8) quantitatively ameliorated both tremor and spasticity in diseased mice. The exacerbation of these signs after antagonism of the CB₁ and CB₂ receptors, notably the CB₁ receptor, using SR141716A and SR144528 (ref. 8) indicate that the endogenous cannabinoid system may be tonically active in the control of tremor and spasticity. This provides a rationale for patients' indications of the therapeutic potential of cannabis in the control of the symptoms of multiple sclerosis², and provides a means of evaluating more selective cannabinoids in the future.

High doses of Δ⁹-tetrahydrocannabinol THC; (the major psychoactive component of cannabis) can inhibit the development of CREAE in rodents^{9,10}, but this has been attributed to immunosuppression preventing the conditions that lead to the development of paralysis, rather than to a direct effect on the paralysis itself^{9,10}. However, the action of cannabinoids on experimental spasticity and tremor remains uncertain because there have so far been no behavioural data on the effects of cannabinoids in animal models relevant to these symptoms of multiple sclerosis.

It is well established that repeated neurological insults occur during CREAE; these are associated with increasing primary demyelination and axonal loss in the central nervous system (CNS)¹. However, it was also evident that CREAE animals can develop additional clinical signs, including unilateral or bilateral fore- and hindlimb tremor (Fig. 1) and hindlimb spasticity (Fig. 2). These accumulate with disease duration and activity. Tremor was associated with voluntary limb movements, but in more severe cases it was persistent at a frequency of ~40 Hz (Fig. 1e). Although considerably faster than encountered in humans (~6 Hz), this frequency is consistent with tremor electromyography in mutant spastic (*Glr^bSp^a*) mice¹¹. These animals develop episodes of rapid tremor and rigidity of the limb and trunk muscles¹². However, unlike the *Glr^bSp^a* mouse, spasticity in CREAE mice need not be triggered by sudden disturbance¹². The effects of cannabis are mediated through the CB₁, CB₂ and putative CB₂-like receptors^{13,14}. CB₁ is predominant in the CNS and is the main target for psychoactivity, but it is also expressed at lower levels in many

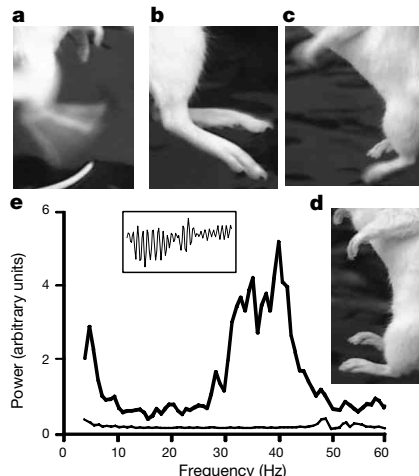


Figure 1 Cannabinoid receptor agonism inhibits tremor in autoimmune encephalomyelitis¹. Mice with hindlimb (a, b) or fore- and hindlimb (c, d) tremor both before (a, c) and after (b, d) treatment with 5 mg kg⁻¹ i.p. with R(+)-WIN 55,212. e, Power spectra of hindlimb tremors recorded with the foot suspended above a strain gauge before (thick line) and after (thin line) 5 mg kg⁻¹ i.p. R(+)-WIN 55,212 injection. Inset, snapshot of raw record over 0.5 s.